Shaping the current waveform of an active filter for optimized system level harmonic conditioning

Espen Skjong[1,3], Marta Molinas[2], Tor Arne Johansen[1] and Rune Volden[3]
[1]*Center for Autonomous Marine Operations and Systems, Department of Engineering Cybernetics, Norwegian University of Science and Technology*
[2]*Department of Engineering Cybernetics, Norwegian University of Science and Technology*
[3]*Ulstein Power & Control AS*
espen.skjong@itk.ntnu.no, marta.molinas@ntnu.no, tor.arne.johansen@itk.ntnu.no, rune.volden@ulstein.com

Keywords: System Level Harmonic Conditioning, Model Predictive Control, Active Filter (AF), Multiple Shooting, Non-linear Loads, Total Harmonic Distortion (THD)

Abstract: Harmonic voltages and currents in electrical systems, when present to a certain degree, represent not only a power quality problem but they are also strongly associated with the electrical system overall losses and they are arguably a source of instability and a safety concern. Mitigating harmonics distortion across the entire system by actively reducing harmonic currents propagation is an effective way of coping with these issues and can be dealt with the injection of a compensating current waveform with an active filter installed at a given bus. This paper shows how, by shaping the compensating current waveform in an optimal way, the overall electrical system harmonic distortion can be optimally reduced in a cost effective manner with a minimum size of the compensating device. The process of shaping this optimal compensating current is shown by how its components are defined by the optimization algorithm using the phase and amplitude of each harmonic as degrees of freedom in the process of finding the optimal waveform. A marine vessel distribution grid is used as representative example to prove the concept.

1 INTRODUCTION

Pure, continuous and constant frequency sinusoidal waveforms are the ideal waveforms in most electric power systems. A given deviation from this ideality is defined as a power quality issue and limits of tolerance are adopted by various standards. Harmonic distortion is one of the possible forms of deviation from a pure sinusoidal waveform. Harmonic distortion is a stationary form of distortion caused by the presence of additional sinusoidal components or harmonics components at multiples of the fundamental frequency component carrying the electrical signal under consideration. Most common sources of these distortions are non-linear loads such as multi (6, 12, 18, 24)-pulse rectifiers, line-commutated converters, high frequency harmonics from voltage source converters (VSC) and switch mode power supplies, saturated transformers and other magnetic components, and power system background voltage distortions (Akagi et al., 2007). These non-linear loads will generally draw a distorted current containing several harmonic components that are multiples of the fundamental frequency component. With a sinusoidal voltage at the source, these harmonic currents will not carry active power to the load but will be circulating as reactive currents in the distribution system and will represent extra distribution losses. One way of approaching this problem is to over-dimension the system to be able to stand the side effects of these harmonics by design. For achieving that, generation, distribution systems and loads will need to be designed over-rated to cope with vibration (generators, motors, transformers), heating and losses originated by these harmonic currents circulating in the system (Evans et al., 2007). This measure however will not alleviate the inherent power quality issues associated with the presence of harmonics which will be reflected at the end-user side. Stability issues in electrical networks have also been correlated with the presence of harmonics (Bing et al., 2007) and reduced stability margins have been reported in association with that. The requirements of power quality standards and safety in electrical installations demand the use of a more active approach when coping with harmonics. Such approach should be aimed at actively reducing the im-

pact of harmonics on power quality by minimizing the total harmonics distortion (THD) using passive or active harmonic filtering techniques. Actively filtering or mitigating the harmonics will have direct implications not only in the quality of the electricity delivered but also in fuel savings, revenues for power transactions, investments in installed capacity of electrical system components, efficient utilization of existing installations and reduction of overall system losses.

Mitigation of harmonics in electrical systems with dispersed generation and loads can be approached by finding the optimum shape of the current wave form that an active filter should inject in a given bus in order to minimize the propagation of harmonics in the entire electrical system. This paper, with references to (Skjong et al., 2015a) and (Skjong et al., 2015b), proposes such an approach based on optimization where the objective is to search for the optimum shape of the current waveform to be injected by an active filter to minimize the THD of the entire electrical system. To prove the concept, the optimization algorithm is implemented in the electrical system of a marine vessel (a discussion of harmonic mitigation using an active filter in a marine vessel's power distribution grid is given in (Rygg Aardal et al., 2015)). The benefits of a system level harmonic mitigation approach is compared with the classical approach of local active filtering. The current waveform shaping process and components resulting from the optimization search are shown for two different loading examples. The component waveforms of the compensating current clearly shows how the optimization algorithm effectively exploits the amplitude and phases of each harmonic component when searching for the optimum waveform shape. A major finding from this research is the possibility to minimize not only the THD of the entire system but to achieve that with the minimum required current rating of the active filter. This will in turn have implications in reducing the investment in the compensating device.

2 POWER DISTRIBUTION GRID MODEL

Power electronics has become the most essential part in modern electrical distribution systems as coupling element between generation, loads and the electrical network as they provide flexibility and fast control capabilities. Most recently, with the emergence of the smartgrid, and due to its inherent properties of fast actuation capabilities and extreme flexibility, power electronics will be critical in the realization of smart grid systems and microgrids which require different voltage levels conversion, frequency conversion capabilities, real-time supply-load match and hybrid AC/DC and DC/AC couplings. Representative examples of these systems are onshore and offshore wind farms connected to a national power distribution network where power electronics in the form of Voltage Source Converters (VSC), High Voltage Direct Current (HVDC) systems, Active Filters (AF), Solid State Transformers (SST), etc., are critical for collecting and distributing the generated power in defined voltage levels and within quality standards. Standalone electrical grids are another example in which power electronics play an essential role in enabling the operation and control of such systems. A standalone microgrid, a wave energy generation plant, an isolated PV generation system and a marine vessel's power distribution grid (Patel, 2011) are typical examples with multiple and dispersed power generation units, e.g. diesel engines, gas turbines, fuel cells and batteries, generating the power needed for different operation scenarios. Despite its enormous advantages, power electronics introduce new non-linear properties and due to its switching mode of operation, it constitutes a source of harmonic distortion in the systems in which they are operating.

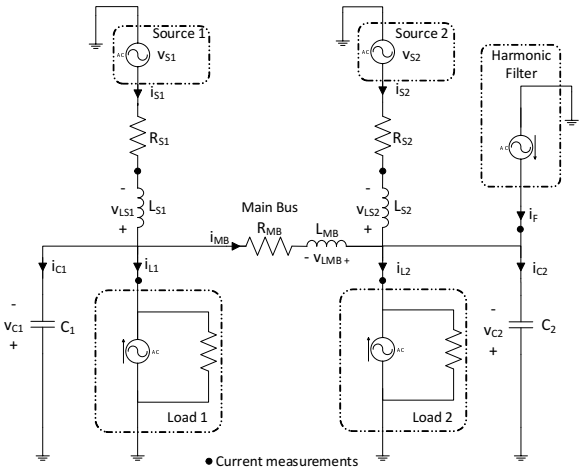

Figure 1: Simplified model of an AC power distribution grid.

In this work a simplified stand-alone power distribution grid is assumed. The power grid, shown in figure 1 with details given in table 1, connects two power sources to two non-linear loads and can resemble a simplified marine vessel microgrid. The loads which can represent the propulsion system are taken as the sources of harmonic pollution in this study. A 6-pulse diode rectifier is considered to be part of the drive system and the harmonic pollution is modelled accordingly. An active harmonic filter based on a

Table 1: Power distribution grid parameters used in case study.

Parameter	Value
L_{S1}	1 mH
L_{S2}	1 mH
L_{MB}	1 mH
R_{S1}	$(0.1 \cdot L_{S1} \cdot \omega)\ \Omega$
R_{S2}	$(0.1 \cdot L_{S2} \cdot \omega)\ \Omega$
R_{MB}	$(0.1 \cdot L_{MB} \cdot \omega)\ \Omega$
C_1	0.1 μF
C_2	0.1 μF

voltage source converter connected to one of the load buses is considered for injecting a compensating current which will be shaped by the optimization algorithm for the purpose of system level harmonic mitigation.

2.1 Model formulation

Considering figure 1 and using Kirchhoff's laws a set of differential equations describing the grid's physical behavior can be derived,

$$\begin{aligned} L_{S1}\frac{di_{S1}}{dt} &= v_{S1} - R_{S1}i_{S1} - v_{C1} \\ C_1\frac{dv_{C1}}{dt} &= i_{S1} - i_{MB} - i_{L1} \\ L_{MB}\frac{di_{MB}}{dt} &= v_{C1} - v_{C2} - R_{MB}i_{MB} \\ C_2\frac{dv_{C2}}{dt} &= i_{MB} + i_{S2} - i_{L2} + i_F \\ L_{S2}\frac{di_{S2}}{dt} &= v_{S2} - R_{S2}i_{S2} - v_{C2}. \end{aligned} \tag{1}$$

The generators are modeled as ideal voltage sources with a voltage phase shift ϕ_V,

$$v_S(t) = \sqrt{2}V_{rms}\sin(\omega t + \phi_V), \tag{2}$$

while the non-linear loads are modeled as current sources with harmonic components of order 5,7,11 and 13 with phase shifts $\phi_{L,i}$ and peak values (amplitudes) $I_{L,i}$,

$$\begin{aligned} i_L(t) &= \sum_i I_{L,i}\sin\left(i\left(\omega t + \phi_{L,i}\right)\right), \\ &\forall i \in \{1, 6k \pm 1 | k = 1,2\}. \end{aligned} \tag{3}$$

The harmonic filter is designed to suppress harmonic pollution and can be modeled as a current source with harmonic components of order 5, 7, 11 and 13,

$$\begin{aligned} i_F(t) &= \sum_i I_{F,i}\sin\left(i\left(\omega t + \phi_{F,i}\right)\right), \\ &\forall i \in \{6k \pm 1 | k = 1,2\}, \end{aligned} \tag{4}$$

where $I_{F,i}$ is the peak values (amplitudes) of the filter's harmonic current component i. The grid model stated above is given as a single phase configuration. A single phase configuration is not a realistic configuration in microgrids, and the equations given above should be extended to a three-phase configuration.

2.2 Three-phase three-wire configuration

Three-phase configurations could consist of three or four wires. The three-phase configuration is modeled using the Clarke transform (Akagi et al., 2007), which converts the *abc* phases to αβ0 phases. Assuming balanced sources the neutral wire (fourth wire) is excessive and the αβ0 frame is simplified to αβ, where the β current is lagging the α current by 90°. Hence, in this work a three-phase three-wire configuration is assumed.

The three-phase three-wire αβ form is derived by extending the single-phase model to three-phase *abc* form. The *abc* form is then transformed to αβ using the Clarke transformation. As an example, the three-phase three-wire model for the voltage sources, assuming balanced sources, can be written in the αβ frame as

$$\mathbf{v}_S(t) = \begin{bmatrix} v_{S,\alpha}(t) \\ v_{S,\beta}(t) \end{bmatrix} = \begin{bmatrix} \sqrt{3}V_{rms}\sin(\omega t + \phi_V) \\ \sqrt{3}V_{rms}\sin(\omega t + \phi_V + \frac{\pi}{2}) \end{bmatrix}. \tag{5}$$

In the same way the load and filter models are extended to three-phase three-wire using the αβ frame, however, the phase shifts $\phi_{L,i}$ and $\phi_{F,i}$ for the filter model and the load models should be equal for the α and β phases due to the definition of the β phase lagging the α phase by 90°. Also the filter amplitudes in the αβ frame are kept equal for each harmonic component when considering balanced loads to ensure a balanced filter.

In the rest of this paper subscript α and β are used to denote the α and β phases for each voltage and current component, and the vectors (phasors) **v** and **i** are used to represents voltages and currents, respectively, given in the αβ frame. It is referred to (Akagi et al., 2007) for details regarding the αβ frame in three-phase three-wire configurations.

2.3 Active Filter (AF) constraints

The harmonic filter model is constrained due to physical limitations of an active filter. The active filter's switching circuit (IGBTs) in conjunction with the rating of the voltage controlled capacitor, decides the active filter's power rating. The IGBT will be the crucial component deciding the filter's current rating, formulated as current limits in the *abc* phases. Figure 2 illustrates the active filter's current limits in both the *abc* and the αβ frames. In the *abc* frame the phases are restricted by

$$i_j^{min} \leq i_j \leq i_j^{max}, \quad \forall j \in \{a,b,c\}, \tag{6}$$

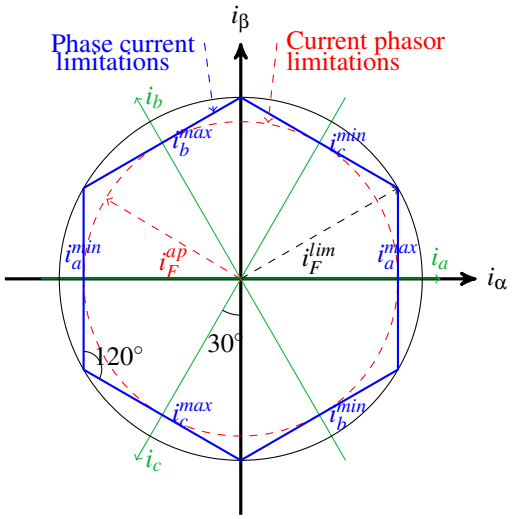

Figure 2: Harmonic filter constraints: Three-phase three-wire represented by the αβ and *abc* frames (Suul, 2012).

which forms the hexagon given in figure 2. These restrictions can be expressed in the αβ frame by

$$-i_F^{lim} \leq -i_{F,\beta} + \frac{\sqrt{3}}{3} i_{F,\alpha} \leq i_F^{lim} \tag{7a}$$

$$-i_F^{lim} \leq i_{F,\beta} + \frac{\sqrt{3}}{3} i_{F,\alpha} \leq i_F^{lim} \tag{7b}$$

$$-i_F^{ap} \leq i_{F,\alpha} \leq i_F^{ap} \tag{7c}$$

$$-i_F^{lim} \leq i_{F,\beta} \leq i_F^{lim}, \tag{7d}$$

where the hexagon's apothem is given by

$$i_F^{ap} = \frac{\sqrt{3}}{2} i_F^{lim}, \tag{8}$$

and i_F^{lim} is a design variable representing the filter's phase current limitations. Eq. (7) gives a set of linear constraints which will be used in an optimization scheme to conduct as much harmonic conditioning as possible for the given power rating. For notational simplicity we define the feasible region for the filter's current vector $\mathbf{i}_F \in \mathbb{S}$.

3 MODEL PREDICTIVE CONTROL

Using the power grid model derived in the previous section an optimization procedure is developed to minimize, by control, the total harmonic currents in the power grid, and prevent harmonic distortions from propagating from the loads to the sources. The optimization procedure is stated as a non-linear model predictive control (NMPC) (Rawlings and Mayne, 2009).

3.1 Formulating the power grid model in standard NMPC form

A NMPC problem for the filter current reference generation in standard form can be stated as

$$\begin{aligned}
&\min_{\mathbf{p},\mathbf{u}} \quad V(\mathbf{x},\mathbf{z},\mathbf{u},\mathbf{p}) = \sum_{n=1}^{N} l(\mathbf{x}_n,\mathbf{z}_n,\mathbf{u}_{n-1},\mathbf{p}) \\
&\text{s.t.} \\
&\dot{\mathbf{x}}_n = \mathbf{f}(\mathbf{x}_n,\mathbf{z}_n,\mathbf{u}_{n-1},\mathbf{p}) \quad \forall n \in \{1,\ldots,N\} \\
&\mathbf{g}(\mathbf{x}_n,\mathbf{z}_n,\mathbf{u}_{n-1},\mathbf{p}) = 0, \quad \forall n \in \{1,\ldots,N\} \\
&\mathbf{h}(\mathbf{x}_n,\mathbf{z}_n,\mathbf{u}_{n-1},\mathbf{p}) \leq 0 | i_{F,n} \in \mathbb{S}, \quad \forall n \in \{1,\ldots,N\} \\
&\text{given initial values } \mathbf{x}_0,\mathbf{z}_0 | \text{initial value } \mathbf{i}_{F,0} \in \mathbb{S},
\end{aligned} \tag{9}$$

where the objective function $V(\cdot)$ and the stage cost function $l(\cdot)$ defines the goal of the optimization. Index n is the time step in the control horizon. The vectors $\mathbf{x},\mathbf{z},\mathbf{u}$ and $\mathbf{p}$ defines the dynamic states, the algebraic states, the controls and the parameters of the problem formulation, respectively. $\mathbf{g}(\cdot)$ represents the problem's equality constraints while $\mathbf{h}(\cdot)$ represents the inequality constraints. Assuming that higher order harmonics (5th, 7th, 11th and 13th) generated by a 6-pulse diode rectifier are known and given by

$$\begin{aligned}
\mathbf{i}_L^{hh} = &\begin{bmatrix} \sum_i I_{L,\alpha,i} \sin\left(i\left(\omega t + \phi_{L,i}\right)\right) \\ \sum_i I_{L,\beta,i} \sin\left(i\left(\omega t + \phi_{L,i} + \frac{\pi}{2}\right)\right) \end{bmatrix}, \\
&\forall i \in \{6k \pm 1 | k = 1,2\},
\end{aligned} \tag{10}$$

the algebraic state vector can be stated as

$$\mathbf{z} = \left[\mathbf{v}_{S1}^\top, \mathbf{v}_{S2}^\top, \mathbf{i}_{L1}^\top, \mathbf{i}_{L2}^\top, \mathbf{i}_F^\top, (\mathbf{i}_{L1}^{hh})^\top, (\mathbf{i}_{L2}^{hh})^\top\right]^\top, \tag{11}$$

where the loads $\mathbf{i}_{L1}$ and $\mathbf{i}_{L2}$ are the three-phase three-wire extension of eq. (3) given in the αβ frame, the filter current $\mathbf{i}_F$ is the three-phase three-wire extension of eq. (4) given in the αβ frame, and the harmonic components of each load, $\mathbf{i}_{L1}^{hh}$ and $\mathbf{i}_{L2}^{hh}$, are given by eq. (10). The dynamic state vector is given by the power grid model's differential states,

$$\mathbf{x} = \left[\mathbf{i}_{S1}^\top, \mathbf{i}_{S2}^\top, \mathbf{i}_{MB}^\top, \mathbf{v}_{C1}^\top, \mathbf{v}_{C2}^\top\right]^\top. \tag{12}$$

The control vector, often referred to as manipulated variables, consists of the active filter's amplitude and phase components,

$$\mathbf{u} = \left[I_{F,\alpha,i}, I_{F,\beta,i}, \phi_{F,i}\right]^\top, \quad \forall i \in \{6k \pm 1 | k = 1,2\} \tag{13}$$

and the parameter vector is given by $\mathbf{p} = 0$. The stage cost function, which should be a convex function, addresses the goal of the optimization, which in this work is to minimize the harmonic pollution in the power grid. A suitable stage cost function is given as

$$\begin{aligned}
l(\mathbf{x},\mathbf{z},\mathbf{u},\mathbf{p}) = &q_1\left(i_{F,\alpha} - i_{L1,\alpha}^{hh}\right)^2 + q_1\left(i_{F,\beta} - i_{L1,\beta}^{hh}\right)^2 \\
&+ q_2\left(i_{F,\alpha} - i_{L2,\alpha}^{hh}\right)^2 + q_2\left(i_{F,\beta} - i_{L2,\beta}^{hh}\right)^2 \\
&+ q_u\left(\mathbf{u}_{I_F}^\top \mathbf{u}_{I_F}\right),
\end{aligned} \tag{14}$$

with constant weights q_1, q_2, q_u, where $\mathbf{u}_{I_F} \subset \mathbf{u}$ that includes the filter's amplitudes. The last part in eq. (14) is added to minimize the filter amplitudes, hence minimizing the filter's power rating, and also providing stability and robustness with regards to modeling errors. $q_u < q_1, q_2$ as minimizing the power rating is of lesser importance than decreasing the harmonic distortion in the power grid.

4 RESULTS

The main objective of this work is to use the NMPC to generate optimized active filter current references by considering the harmonic pollution from both loads and utilizing filter current amplitudes and phases as control variables. Two case studies are proposed, one with symmetric and one with asymmetric loads. In both cases the loads introduce a high level of harmonic pollution in form of the 5th, 7th, 11th and 13th harmonic components, and the active filter currents are limited to $i_F^{lim} = 0.5$ [pu] ($i_F^{ap} = \frac{\sqrt{3}}{4}$ [pu]). The load currents for both study cases are presented in table 2. A local filter reference generation (local filtering) considering only load 2 is implemented for comparison purposes. It is important to remark that the local filtering does not consider the filter's physical limits and generates filter currents exactly mimicking the harmonic currents from load 2 with a phase shift of 180°. The fundamental frequency is fixed to $f = 50$ [Hz] in both study cases.

4.1 Symmetric Loads

Figure 3 and 4 represents the simulation results for case 1 in table 2. The upper plot in figure 3(a) represents the NMPC filter current and local filtering current in the *a* phase. The local filtering current is the saturated load 2 harmonics phase shifted 180°. By comparing the two filter currents one clearly see that the NMPC filter current has different amplitudes from the local filtering current, and at approximated time instances 0.0025 and 0.0175 [s], among others, the NMPC filter current's phases (one phase for each harmonic component) have been altered, which is seen as a deviation from the local filter current's visual representation.

The four lower plots in figure 3(a) represent the load voltages (*a* phase) and respective frequency spectra's with calculated THD values. Due to numerical errors related to discretization, the THD values are calculated based on a frequency spectrum in a range of 0-650 [Hz]. With either filtering technique the THD of load 2 voltage is lower than load 1. This is as expected since the active filter is installed near load 2. Hence the load 1 voltage will in either case be more distorted than the load 2 voltage due to the inductance in the main bus preventing the filter to perfectly compensate for all the harmonics generated by load 1 and 2. As can be seen, the THD values from local filtering is higher compared to the NMPC case. First of all, the local filtering does not take into consideration the filter's limitation and load 1 harmonics, and the compensating filter current using this filtering technique would be the 180° phase shifted load 2 harmonics. However, the filter is too small to cope with the distorted grid, which means the filter will saturate the calculated filter current references from local filtering resulting in a THD value for load 1 almost as high as without filtering (19.5%). The NMPC, however, takes into account both loads and also the filter limits in the calculation of optimal filter current references. This way the filter current references will not be saturated due to exceeding the active filter's physical limits.

Figure 3(b) represents the filter current (phase *a*) frequency spectra for both NMPC and local filtering. As can be seen, the amplitudes for the dominant frequency components are generally lower for the NMPC filter current than for the local filtering current. The filter current were modeled by the 5th, 7th, 11th and 13th harmonic component, which represents frequencies of 250, 350, 550 and 650 [Hz]. As evident from the plot, other frequency components are utilized by the NMPC due to the ability to rapidly manipulate the harmonic components' phases. Due to the saturation of the local filtering current other harmonic components than those modeled are also present in the frequency spectra.

Figure 4 represents the 5th, 7th, 11th and 13th harmonic components of the NMPC filter current and local filtering current in the *a* phase. From this representation it is easy to show that the NMPC does utilize both, the amplitudes and the phases of each modeled harmonic component in the filter reference current. The load 2 current, which also represents the unsaturated reference current from local filtering, and the NMPC do share the same fundamental frequency, but due to the utilization of the harmonic phases the NMPC filter current components are completely changed and it is not easy to determine neither frequency nor period from the plots. One important finding is the total magnitude of each harmonic filter current component. As can be seen, the filter current components, in this case, do not increase beyond 0.12 [pu]. Compared to the local filtering, utilization of filter current phases would be an important degree of freedom when coping with high harmonic pollu-

Table 2: Study case configurations.

	Load 1 amplitudes [1th, 5th, 7th, 11th, 13th]	**Load 2 amplitudes** [1th, 5th, 7th, 11th, 13th]	**Load 1 phases** [1th, 5th, 7th, 11th, 13th]	**Load 2 phases** [1th, 5th, 7th,11th, 13th]
Case 1 (symmetric)	$I^{\alpha}_{L1} = I^{\beta}_{L1} = [0.9, 0.6, 0.3, 0.5, 0.8]$	$I^{\alpha}_{L2} = I^{\beta}_{L2} = [0.9, 0.6, 0.3, 0.5, 0.8]$	$\phi_{L1} = [0, 0, 0, 0, 0]$	$\phi_{L2} = [0, 0, 0, 0, 0]$
Case 2 (asymmetric)	$I^{\alpha}_{L1} = I^{\beta}_{L1} = [0.9, 0.8, 0.6, 0, 0.5]$	$I^{\alpha}_{L2} = I^{\beta}_{L2} = [0.9, 0, 0.6, 0.8, 0]$	$\phi_{L1} = [0, 0, 0, 0, 0]$	$\phi_{L2} = [0, 0, 0, 0, 0]$

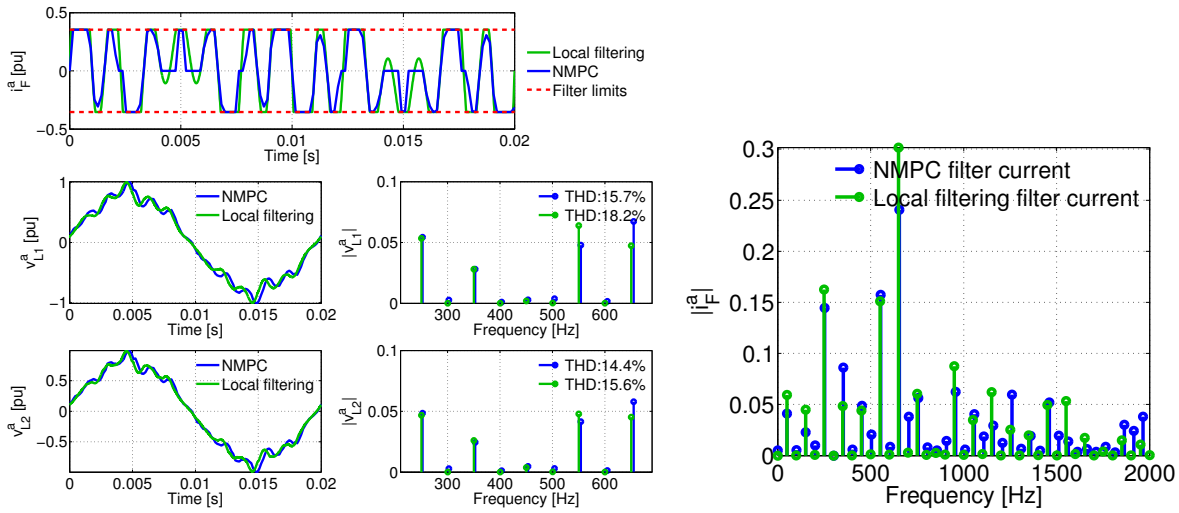

(a) Filter currents and load voltages.

(b) Filter current spectrum.

Figure 3: Case 1 (symmetric loads): Filter currents and filtered load voltages.

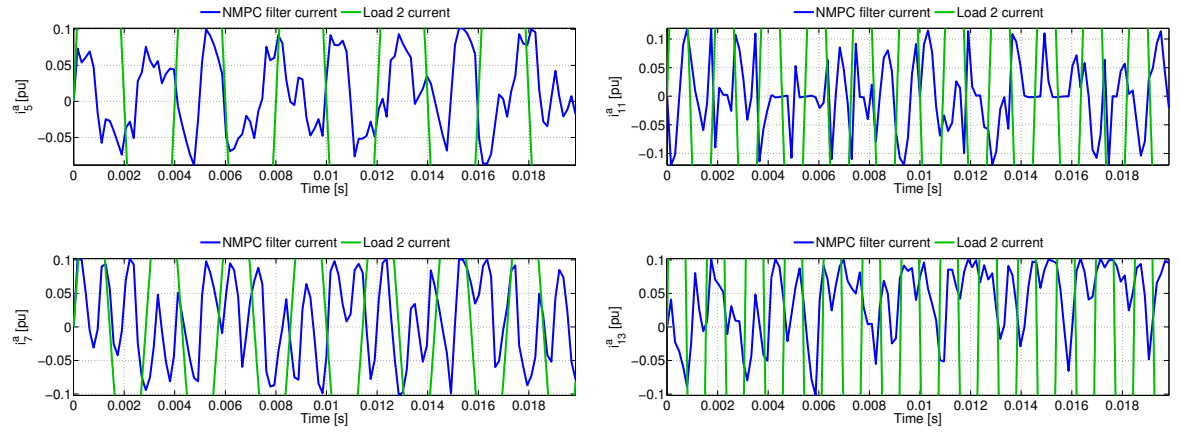

(a) 5th and 7th filter current component.

(b) 11th and 13th filter current component.

Figure 4: Case 1 (symmetric loads): Filter current components.

tions using a relative small active filter. Active filters are generally quite expensive, thus increasing the filter size could be a costly affair.

4.2 Asymmetric Loads

Figure 5 and 6 represents the simulation results for case 2 in table 2. The upper plot in figure 5(a), as in the previous case, represents the NMPC filter current and the local fingering current in the a phase. In this case the NMPC filter current is more phase shifted, compared to the local filtering current, than in the synchronous loads case. This is a direct consequence of the optimization trying to condition both load currents. The phase shifting, compared to local filtering, is illustrated at, among others, approximated time instances 0.002 and 0.008 [s].

The four lower plots in figure 5(a) shows that the

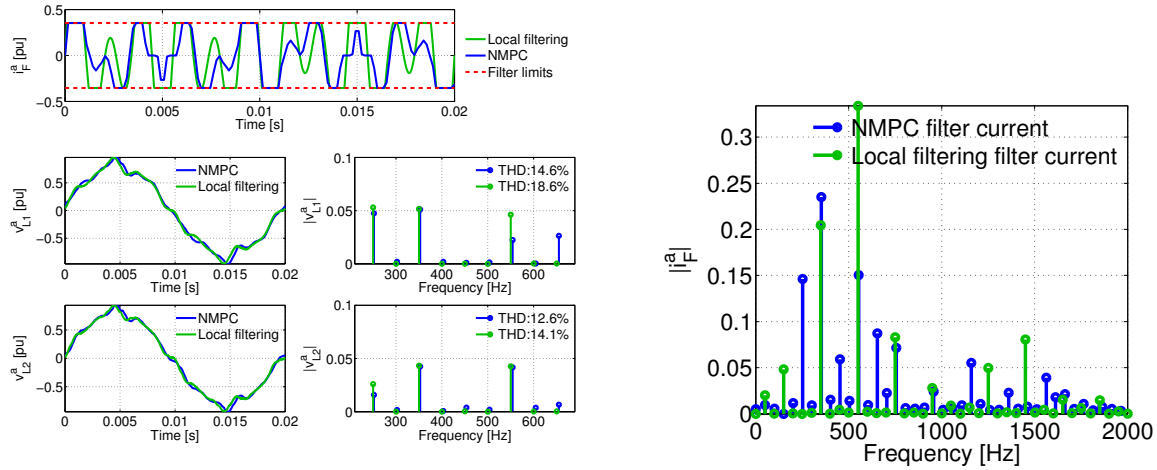

(a) Filter currents and load voltages.

(b) Filter current spectrum.

Figure 5: Case 2 (asymmetric loads): Filter currents and filtered load voltages.

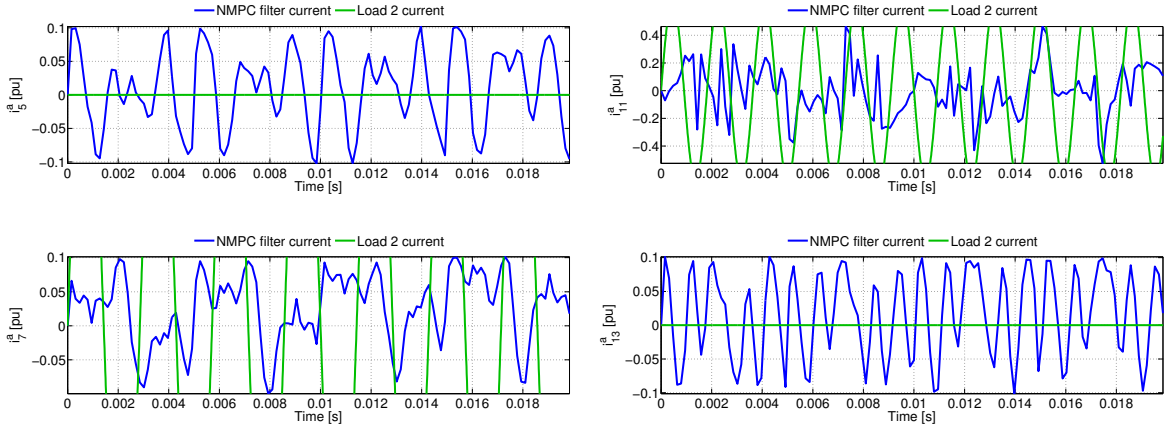

(a) 5th and 7th filter current component.

(b) 11th and 13th filter current component.

Figure 6: Case 2 (asymmetric loads): Filter current components.

differences in THD for NMPC and local filtering are higher in the asymmetric case than in the symmetric case. This is due to the NMPC's consideration of all loads, whereas local filtering does only consider load 2. Also, the filter limits saturate the local filter currents, as pointed out in the previous case, preventing the filter from conducting the intended filtration. Compared with no filtering for v_{L1} (21.1%) the local filtering approach performs poorly. The NMPC avoids filter current saturation by considering the filter limits and by utilizing the filter current amplitudes and phases to make the best possible harmonic conditioning out of the filter.

Figure 5(b) showcases the filter current (phase a) frequency spectra for both NMPC and local filtering. The discussion and analysis from the symmetric case is also applicable for the asymmetric case. In general, dominant current amplitudes are smaller in the case of NMPC than for local filtering. However, the NMPC utilizes the filter current phases to utilize un-modeled frequency components with its cause of lowering the filter current amplitude. This is seen in the figure where amplitudes of the frequency components, apart from the 5th, 7th, 11th and 13th, are generally higher for the NMPC case than for local filtering. Due to the configuration of the asymmetric loads, which for the loads combined includes all modeled frequency components, the NMPC will represent harmonic components present in both loads. This can be seen in the 5th component (250 [Hz]), whereas the NMPC has a non-zero amplitude compared with the local filtering's zero amplitude.

The 5th, 7th, 11th and 13th harmonic components of the NMPC's filter current in phase a are showcased

in figure 6 compared with the load 2 current in the same phase. As can be seen from the configuration in table 2 and from the figure, the 5th and 13th harmonic component in load 2 are zero. However, due to asymmetric loads all NMPC filter current components are utilized. This is due to the fact that load 1 and 2 combined represents all modeled harmonics polluting the grid. As with the symmetric case, the NMPC filter current components are non-periodic due to the rapid utilization of the filter amplitudes and phases for each harmonic component. As a result of rapidly altering the phases and amplitudes for each harmonic component, the amplitudes can be kept small, which is illustrated in figure 6 where none of the filter components reach a higher amplitude than 0.1 [pu]. As a result of the utilization of amplitudes and phases for each modeled harmonic component, the NMPC could also prevent un-modeled harmonics from polluting the grid. This is a useful property specially when simple grid models are available for a real-time implementation of the optimization scheme.

5 CONCLUSION

A non-linear model predictive controller (NMPC) applied to system level harmonic conditioning in a generalized power grid has been outlined and discussed in detail. Two different study cases were presented. A local filtering procedure was introduced to compare with the NMPC filter reference current generation approach and to highlight the benefits of system level harmonics mitigation.

The NMPC was able to achieve better harmonic conditioning than the local filtering due to the consideration of both loads and the active filter's physical limits. The NMPC's ability to rapidly alter the amplitudes and phases of each modeled harmonic components in the filter current gave flexibility in terms of un-modeled harmonic components present in the loads, the ability to optimize the harmonic mitigation with limited filter's size and distortions from both loads. The NMPC's ability to alter the phases and amplitudes of each harmonic filter current component is important when un-modeled harmonic frequency components are present in the loads, and a simple power grid model could be enough to obtain a real-time implementation of the NMPC. Compared with the local filtering, the NMPC was not affected by saturation of the filter current references. The saturation of the local filtering resulted in higher THDs. With the system level harmonics mitigation approach, the NMPC was able to optimize the active filter current to achieve the best possible harmonic conditioning for both load currents with a given filter's physical limitations.

ACKNOWLEDGEMENT

This work has been carried out at the Centre for Autonomous Marine Operations and Systems (AMOS), supported by Ulstein Power & Control AS and The Norwegian Research Council, project number 241205.

REFERENCES

Akagi, H., Watanabe, E., and Aredes, M. (2007). *Instantaneous Power Theory and Applications to Power Conditioning*. IEEE Press Series on Power Engineering. Wiley.

Bing, Z., Karimi, K., and Sun, J. (2007). Input impedance modeling and analysis of line-commutated rectifiers. In *IEEE Power Electronics Specialists Conference, 2007. PESC 2007*, pages 1981–1987.

Evans, I., Hoevenaars, A., and Eng, P. (2007). Meeting harmonic limits on marine vessels. In *Electric Ship Technologies Symposium, 2007. ESTS '07. IEEE*, pages 115–121.

Patel, M. (2011). *Shipboard Electrical Power Systems*. Shipboard Electrical Power Systems. Taylor & Francis.

Rawlings, J. and Mayne, D. (2009). *Model Predictive Control: Theory and Design*. Nob Hill Pub.

Rygg Aardal, A., Skjong, E., and Molinas, M. (2015). Handling system harmonic propagation in a diesel-electric ship with an active filter. In *ESARS 2015 Conference on Electrical Systems for Aircraft, Raukway, Ship Propulsion and Road Vehicles*.

Skjong, E., Molinas, M., and Johansen, T. A. (2015a). Optimized current reference generation for system-level harmonic mitigation in a diesel-electric ship using non-linear model predictive control. In *IEEE 2015 International Conference on Industrial Technology, ICIT.*

Skjong, E., Ochoa-Gimenez, M., Molinas, M., and Johansen, T. A. (2015b). Management of harmonic propagation in a marine vessel by use of optimization. In *IEEE Transportation Electrification Conference and Expo 2015 (ITEC).*

Suul, J. A. (2012). *Control of Grid Integrated Voltage Source Converters under Unbalanced Conditions*. PhD thesis, Norwegian University of Science and Technology, Department of Electrical Power Engineering.